Rapid Communications

Integer quantum Hall transition on a tight-binding lattice

Martin Puschmann,[1] Philipp Cain,[2] Michael Schreiber,[2] and Thomas Vojta[1]
[1]*Department of Physics, Missouri University of Science and Technology, Rolla, Missouri 65409, USA*
[2]*Institute of Physics, Chemnitz University of Technology, 09107 Chemnitz, Germany*

(Received 27 November 2018; published 19 March 2019)

Even though the integer quantum Hall transition has been investigated for nearly four decades its critical behavior remains a puzzle. The best theoretical and experimental results for the localization length exponent ν differ significantly from each other, casting doubt on our fundamental understanding. While this discrepancy is often attributed to long-range Coulomb interactions, Gruzberg *et al.* [Phys. Rev. B **95**, 125414 (2017)] recently suggested that the semiclassical Chalker-Coddington model, widely employed in numerical simulations, is incomplete, questioning the established central theoretical results. To shed light on the controversy, we perform a high-accuracy study of the integer quantum Hall transition for a microscopic model of disordered electrons. We find a localization length exponent $\nu = 2.58(3)$ validating the result of the Chalker-Coddington network.

DOI: 10.1103/PhysRevB.99.121301

The discovery of the integer quantum Hall (IQH) effect by Klitzing *et al.* [1] opened a new area in condensed matter physics, combining topology and Anderson localization. Two-dimensional electrons in a perpendicular magnetic field B follow circular cyclotron orbits that are quantized into discrete *Landau levels* (LLs), having energies $E_n = (n + 1/2)\hbar\omega$, with integer n and cyclotron frequency $\omega = eB/m$. Disorder broadens each LL into a Landau band (LB) and localizes all electronic states in the bulk except for a single energy in each band center [Fig. 1(a)]. At the system rim, skipping cyclotron orbits lead to edge states [Fig. 1(b)] that are extended along the boundary even in the presence of disorder and cause the plateau structure of the Hall conductance. Quantum Hall states are thus examples of topological insulators, bulk insulators with protected edge states. When the Fermi energy is tuned through one of the critical states, the system undergoes a quantum phase transition between two localized phases. This IQH transition belongs to the realm of Anderson transitions, and the critical exponent ν describes the divergence $\xi \sim |E - E_c|^{-\nu}$ of the localization length ξ at the IQH critical point E_c [2,3].

Critical scaling at the IQH transition has been observed in various systems [4–6]. Recent experiments on $Al_xGa_{1-x}As$ heterostructures [5] measure ν and the dynamical exponent z independently of each other, giving $\nu = 2.38(5)$ and $z = 1$. While early numerical investigations of the IQH transition provided ν values from 2.3 to 2.4 [7–13], newer high-accuracy studies based on the semiclassical Chalker-Coddington (CC) network model yielded significantly larger values $\nu \approx 2.60$ with small errors of about 0.02 [14–21]. The disagreement between the best experimental and theoretical values casts doubt on our fundamental understanding of IQH transitions. How can this exponent puzzle be solved? One candidate is the Coulomb interaction that is not included in the simulations but clearly present in real materials [5,6,9,22–27]. However, Gruzberg *et al.* [28] recently questioned the validity of the semiclassical CC network even within the single-particle framework. They suggested that the CC network is too regular and does not contain all types of disorder relevant at the IQH transition. For a modified network model, they observed $\nu \approx 2.37$, remarkably close to the experimental value. A recent study of the quantum Hall problem in the presence of δ-impurity potentials gave $\nu = 2.4(1)$ [29], and a Chern number calculation obtained $\nu = 2.48(2)$ [30], adding to the controversy.

In this Rapid Communication, we address this controversy by studying the IQH transition in a microscopic tight-binding model of noninteracting electrons on a square lattice. We perform a careful finite-size scaling analysis for large systems of up to 768×10^6 lattice sites. In the universal regime, where neither LL coupling nor the nonzero intrinsic LL width affect the transition, we find $\nu = 2.58(3)$, in agreement with the (standard) CC network. Thus, the discrepancy between theory and experiment persists even for a microscopic model of noninteracting electrons, pointing to the Coulomb interactions as main culprit.

In the rest of this Rapid Communication, we introduce our model and the numerical method. We then present our results and compare them with Refs. [28–30]. We conclude by discussing broader implications for the IQH transition.

We consider a square-lattice tight-binding model of noninteracting electrons in a perpendicular magnetic field $\mathbf{B}$. The Hamiltonian, a generalization of the Anderson model of localization, reads

$$\mathbf{H} = \sum_j u_j |j\rangle\langle j| + \sum_{\langle j,k\rangle} \exp(i\varphi_{jk}) |j\rangle\langle k|. \tag{1}$$

Here, $|j\rangle$ denotes a Wannier orbital on site j. The potentials u_j are independent random variables drawn from a uniform distribution in the interval $[-W/2, W/2]$, characterized by disorder strength W. The hopping terms between nearest neighbors $\langle j, k\rangle$ have a constant magnitude but complex phase shifts induced by the magnetic field [31,32]. Choosing the Landau gauge for the vector potential, $\mathbf{A} = (0, Bx, 0)$, the

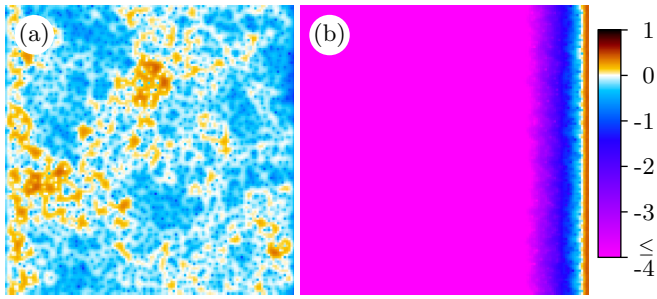

FIG. 1. Critical state (left, $E = E_c = 3.4221$) and edge state (right, $E = 3.0056$) for a square system of linear size $L = 128$, magnetic flux $\Phi = 1/10$, and disorder strength $W = 0.5$. Coloring represents wave-function intensities $|\psi_j|^2$ at site j via $\log_{L^2}(L^2|\psi_j|^2)$. Periodic and open boundary conditions are applied in the y and x directions, respectively.

Peierls phases read

$$\varphi_{jk} = \frac{e}{\hbar}\int_j^k \mathbf{A}\cdot d\mathbf{r} = \begin{cases} 0, & \text{in the } x \text{ direction,} \\ \pm 2\pi\Phi x_j, & \text{in the } \pm y \text{ direction,} \end{cases} \tag{2}$$

where x_j is the x coordinate of site j in units of the lattice constant l. $\Phi = Bl^2e/h$ is the magnetic flux through a unit cell in units of the flux quantum h/e.

Without disorder, $W = 0$, the energy spectrum of the Hamiltonian (1) is fractal and takes the form of the famous Hofstadter butterfly [33,34] (see Fig. 2). The spectrum is symmetric with respect to energy $E = 0$, reflecting the bipartite character of the lattice. The spectrum is also periodic in Φ with period 1 and symmetric with respect to $\Phi = 1/2$. For a rational $\Phi = p/q$ with coprime integers p and q, the spectrum splits into exactly q LLs [35]. In contrast to the free-electron gas, each LL has a *nonzero intrinsic width*. For small Φ and small LL indices n, the spectra become similar to LLs of free electrons; i.e., their widths vanish, and their energies

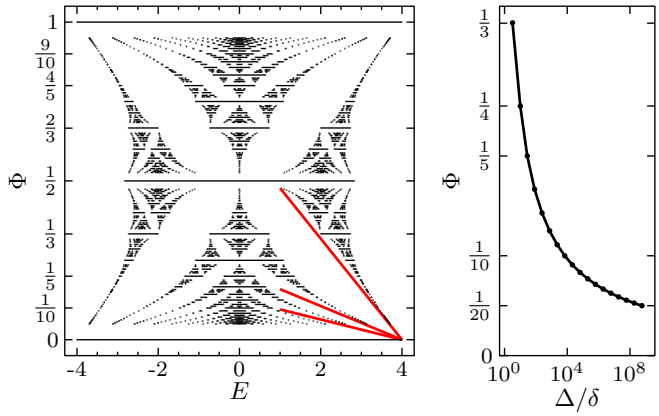

FIG. 2. Left: Hofstadter butterfly. Energy spectrum of Hamiltonian (1) in the clean case ($W = 0$). For $\Phi = 0$ and 1, there is a single band from $E = -4$ to 4. Landau levels are shown for $\Phi = p/q$ with coprime numbers $p, q \leqslant 20$. The free-electron approximation (solid red lines), $E_n^+ = 4 - 4\pi\Phi(n + 1/2)$, is shown for $n = 0$, 1, and 2. Right: LL spacing (midband distance Δ between the LLs with $n = 0$ and $n = 1$) in multiples of the intrinsic LL width δ as a function of Φ.

follow $E_n^\pm = \pm 4 \mp 4\pi\Phi(n + 1/2)$, where $\pm$ distinguishes the positive and negative sides of the spectra.

Random potentials, $W > 0$, broaden the LLs further, and all extended states turn into localized states except for one critical state in each LL that shows multifractal fluctuations. To determine the universal properties of the IQH transition, we need to consider parameters for which neither LL coupling nor the intrinsic LL width play a role. The disorder must thus lead to LL broadening that is larger than the intrinsic LL width δ but smaller than the LL spacing Δ. The dependence of δ and Δ on Φ is presented in the right panel of Fig. 2, demonstrating that both conditions are easily fulfilled for small Φ, where $\Delta/\delta \gg 1$. However, the magnetic length $L_B = \sqrt{(2n+1)/(2\pi\Phi)}$ becomes large for small Φ, making the effective system size L/L_B too small. Hence, we expect the numerically most favorable situation for the lowest LL, $n = 0$, and moderate Φ.

We analyze the electronic states via the recursive Green's function algorithm [36–38]. It considers a quasi-one-dimensional strip of $L \times N$ sites ($N \gg L$) which is divided into layers of $L \times 1$ sites. The Green's function $\mathbf{G} = [(E + i\eta)\mathbf{I} - \mathbf{H}]^{-1}$ is calculated iteratively layer by layer, and the smallest positive Lyapunov exponent γ derives from the Green's function between the two strip ends, i.e., between the layers $x_j = 1$ and $x_j = N$ [39],

$$\gamma = -\lim_{N\to\infty}\lim_{\eta\to 0}[\ln \mathrm{tr}|\mathbf{G}_{1,N}|^2/(2N)]. \tag{3}$$

We consider strips along the x direction so that periodic boundary conditions in the layer direction do not restrict the value of Φ. We determine the critical behavior by finite-size scaling of the dimensionless Lyapunov exponent $\Gamma \equiv \gamma L$ for varying strip width L. Our $\Gamma(E, \Phi, L)$ data are averages of 50 strips with $L \leqslant 512$ and length $N = 10^6$ for each E and Φ. For $\Phi = 1/10$, we increase the accuracy by using $L \leqslant 768$ and 150–200 strips. The relative statistical uncertainties of Γ scale approximately with $\sqrt{L}$ and range from 0.0003 for $L = 16$ to 0.0022 for $L = 768$. We use an imaginary energy $\eta = 10^{-14}$ to approximate the limit $\eta \to 0$.

With this method, we study the lowest LB for flux $\Phi = 1/3$, 1/4, 1/5, 1/10, 1/20, 1/100, and 1/1000 [40]. (We consider ratios of the form $1/q$ to avoid splitting of the LB into subbands.) For each Φ, we choose a disorder strength W such that $\delta < W \lesssim \Delta$. Details of the simulation parameters are provided in the Supplemental Material [41], which also shows the resulting density of states for several Φ. For reliable results, we analyze the critical behavior of the Lyapunov exponent Γ in two ways: First, we analyze the energy and system-size dependencies of Γ graphically. Then we apply compact, sophisticated scaling functions to our data.

The location of the transition, i.e., the critical energy E_c, is identified as the position of the minimum of Γ with respect to E (see Fig. 3). Figure 4 shows the L dependence of Γ at the minimum position $E_{\min}$ for several Φ (where $E_{\min} \to E_c$ for $L \to \infty$). Expressing the strip width L in multiples of the magnetic length $L_B = 1/\sqrt{2\pi\Phi}$, all data line up for small $\Phi \lesssim 1/10$. We conclude that these data are unaffected by LL coupling and the nonzero LL width and thus represent the universal behavior of the IQH transition. For $\Phi = 1/5$, the increased intrinsic LL width, $\Delta/\delta \approx 28$, leads to deviations, but

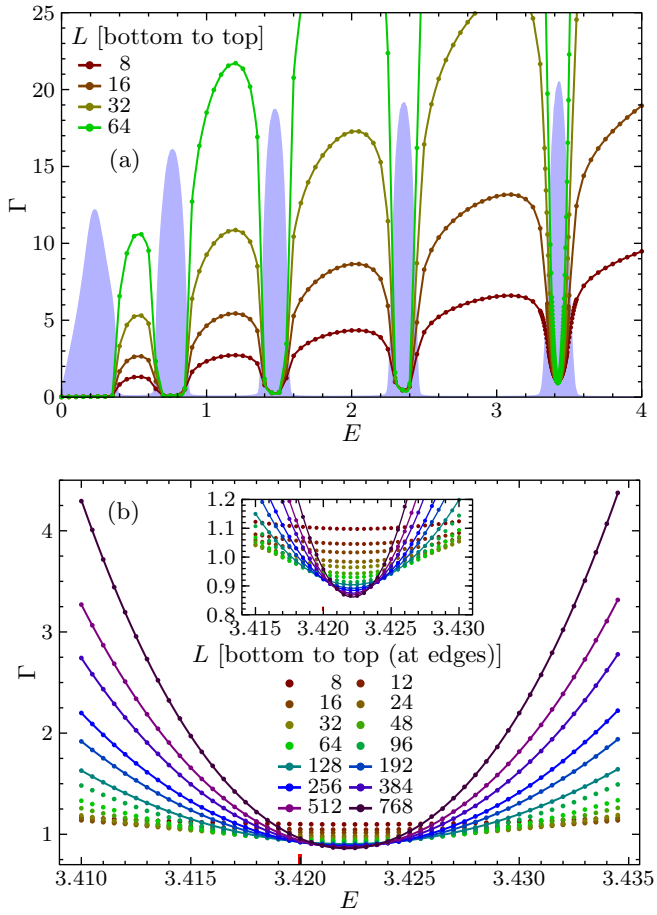

FIG. 3. (a) Dimensionless Lyapunov exponent $\Gamma(E, L)$ for $\Phi = 1/10$ and $W = 0.5$ as a function of E for several L. The statistical errors are well below the symbol size. The blue area shows the density of states in arbitrary units. Lines are guides to the eye only. (b) $\Gamma(E, L)$ close to the lowest IQH transition. The solid lines are fits (see main text for details). The inset shows the immediate vicinity of the transition. The tiny red bar at the bottom shows the energy range of the LL in absence of disorder (compare Fig S1).

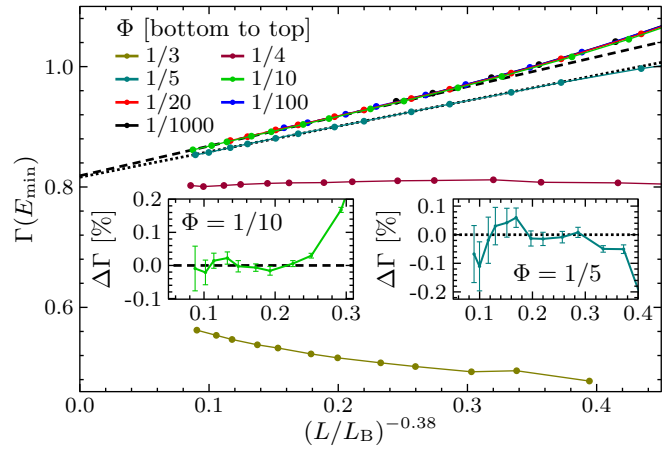

FIG. 4. System-size dependence of Γ at $E_{\min}$ for several Φ under assumption of an irrelevant exponent $y = 0.38$. The fits of Eq. (4) for $\Phi \leqslant 1/10$ (black dashed line) and $\Phi = 1/5$ (black dotted line) are based on the data with $L \geqslant 128$. The statistical errors are below the symbol size. The insets show the deviations $\Delta\Gamma$ of the data points from the fit functions. Solid lines are guides to the eye only.

the asymptotic behavior seems to be similar to the universal case. For higher Φ, the modifications are stronger, indicating nonuniversal behavior. In the following, we therefore focus on the universal regime, $\Phi \lesssim 1/10$.

The strong size dependence of the critical Lyapunov exponent implies that corrections to scaling are important. We provide a comprehensive discussion of finite-size corrections in the Supplemental Material [41]. In the simplest case, they follow a power law,

$$\Gamma(E_c, \Phi, L) = \Gamma_c[1 + a(L/L_B)^{-y}], \tag{4}$$

with an irrelevant exponent $y > 0$. In the literature, estimates of y vary widely between $y \approx 0.15$ [15,21] and $y \approx 0.6 \ldots 0.8$ [20,28,42]. y values at both ends of this range do not describe our data in the universal regime. However, a midrange value, $y = 0.38$ [16,20,43], correctly describes the behavior from $L \approx 44L_B$ to our largest sizes of $L \approx 608L_B$, yielding $\Gamma_c = 0.818(1)$. We also consider the possibility that the leading corrections to scaling take a logarithmic form $\Gamma = \Gamma_c\{1 + a/\log[\lambda(L/L_B)]\}$ (with unknown scaling factor scale λ) [18,21]. Our universal data ($\Phi \leqslant 1/10$) for $L \geqslant 20L_B$ agree well with the logarithmic form, giving $\Gamma_c = 0.738(1)$ and $\lambda = 1.68(4)$.

Besides $\Gamma(E_c)$, we analyze the curvature $\Gamma''(E_c)$ which is supposed to scale as $L^{2/\nu}$ for large L. Figure S3 in the Supplemental Material [41] shows $\Gamma''(E_c)$ as a function of L/L_B. Again, all data for $\Phi \lesssim 1/10$ line up, confirming the universal regime. Moreover, the graphical analysis provides strong evidence for the asymptotic ν to be significantly above 2.4.

For reliable quantitative estimates, we now focus on fits of a sophisticated scaling function $\Gamma(x_r L^{1/\nu}, x_i L^{-y})$ that provide estimates for all critical parameters, i.e., Γ_c, ν, and y, simultaneously. In the Supplemental Material [41], we describe in detail this function and its expansion in terms of the relevant scaling field $x_r L^{1/\nu}$ and irrelevant scaling field $x_i L^{-y}$ with scaling variables $x_r(E - E_c)$ and $x_i(E - E_c)$. Based on the above discussion, a flux of $\Phi = 1/10$ is most suitable to obtain high-accuracy critical parameters, because (i) the data fall onto the universal master curve in Fig. 4, and (ii) we can still reach large effective sizes up to $L = 608L_B$.

Figure 3(b) shows Γ with 50 energies close to E_c for each L. We obtain the best fits by neglecting smaller systems, $L < 128$, and including the leading order of the irrelevant scaling field only. This yields $E_c = 3.422\,151(3)$ and $\Gamma_c = 0.814(6)$ with critical exponents $\nu = 2.594(14)$ and $y = 0.357(26)$. Neglecting further systems leads to consistent results but increased uncertainties. Without irrelevant corrections, we observe $\nu = 2.595(12)$ based on the two largest systems. To extend the fit to smaller systems, higher correction orders are needed, but the estimates become less reliable. Based on the robustness of the results with respect to the system-size range and fit expansions, we estimate the critical parameters to be $\Gamma_c = 0.815(8)$, $\nu = 2.58(3)$, and $y = 0.35(4)$, as explained in Ref. [41]. We perform analogous fits for the logarithmic correction-to-scaling scenario. Employing an irrelevant scaling field $x_i/(b + x_i \log L)$ in our scaling ansatz for Γ leads to

$\Gamma_c = 0.745(6)$, $\nu = 2.597(27)$ for $L \geqslant 128$. Including smaller systems requires higher-order corrections, giving $\Gamma_c \approx 0.74$ and $\nu \approx 2.60$ with increased uncertainties.

For fluxes $\Phi < 1/10$, the effective sizes L/L_B are smaller, leading to more pronounced finite-size effects. If higher expansion orders of the irrelevant scaling field are included in the fit, we still find values $\nu \approx 2.56$ and $y \approx 0.38$ for $\Phi = 1/20$ and $1/100$. However, for $\Phi = 1/1000$, our largest system size $L = 512$ corresponds to $41L_B$ only, and our critical parameters, i.e., $\Gamma_c \approx 0.89$, $\nu \approx 2.35$, and $y \approx 0.7$, differ significantly from the above values. This clearly shows that a size of $41L_B$ is too small to describe the asymptotic behavior.

For larger fluxes $\Phi > 1/10$, the intrinsic LL width is comparable to the LL spacing. These transitions are not expected to be in the universal regime. Still, for $\Phi = 1/5$, the asymptotic behavior seems to be similar to that of the universal curve (see Fig. 4), and our finite-size scaling analyses provide compatible results. However, for higher Φ, deviations are much stronger (see the Supplemental Material [41]).

In summary, we have studied the IQH transition in the lowest LL of a microscopic model of noninteracting electrons. In the universal regime where neither the intrinsic LL width nor LL coupling play a role, we find a localization length exponent of $\nu = 2.58(3)$, independent of the details of the finite-size scaling analysis. Based on our data, we cannot discriminate between power-law corrections to scaling with an irrelevant exponent $y = 0.35(4)$ and logarithmic corrections.

Our localization length exponent agrees well with recent high-accuracy results of the standard CC model [15–18,20,21]. Our estimates for the critical Lyapunov exponent depend on the correction type: We found $\Gamma_c = 0.815(8)$ and $\Gamma_c = 0.745(6)$ for power-law and logarithmic corrections, respectively. In both cases, our estimates are slightly larger (by about 0.025) than those of transfer-matrix calculations on the CC network model [15,18,21]. However, using $\Gamma_c = \pi(\alpha_0 - 2)$ [44], $\Gamma_c = 0.815(8)$ corresponds to the multifractal exponent $\alpha_0 = 2.2594(15)$ which coincides with $\alpha_0 = 2.2596(4)$ [45] and $2.2617(6)$ [46] found for the CC network model.

Our results suggest that the discrepancy between the experimental and theoretical values of ν cannot be attributed to a too regular structure of the semiclassical CC network model [47]. Why did the modified CC network [28], the Chern number calculation [30], and the IQH transition study in the presence of δ impurities [29] lead to different critical behavior with smaller ν? The latter two investigations used linear system sizes up to about $100L_B$, much smaller than our largest sizes of more than $600L_B$. Moreover, corrections to scaling were not included in the analysis of Ref. [29] or are apparently almost negligible in Refs. [30,48]. We therefore believe that the system sizes may be too small to reach the asymptotic regime. (In our system the crossover to the asymptotic behavior occurs for $L \gtrsim 110L_B$.) Insufficiently small system sizes are also assumed to be the reason why early numerical studies gave ν values in the range of 2.3–2.4 [49] (see Fig. S3 in the Supplemental Material [41]).

The modified CC network case is less clear, as the system sizes in Ref. [28] are comparable to sizes used in recent studies of the standard CC network. Does the deviation between $\nu \approx 2.37$ found in Ref. [28] and $\nu \approx 2.60$ in our model and the standard CC network mean that they belong to different universality classes? We note that the modified CC network of Ref. [28] has much stronger corrections to scaling [a stronger size dependence of $\Gamma(E_c)$]. This may push the crossover to the asymptotic regime to larger sizes. Establishing the universality class of the modified CC model remains a task for the future.

In conclusion, our results imply that the paradigmatic CC network model correctly captures the physics of disordered noninteracting electrons close to the IQH transition, in contrast to what was suggested in Ref. [28]. Electron-electron interactions thus remain the likely culprit for the puzzling disagreement between the best theoretical and experimental results for the critical behavior. Whereas screened interactions were shown to be irrelevant at the noninteracting fixed point, long-ranged Coulomb interactions are believed to be relevant [10]. However, quantitative results for the critical behavior in the presence of Coulomb interactions do not exist.

This work was supported by the NSF under Grants No. DMR-1828489, No. DMR-1506152, No. PHY-1607611, and No. PHY-1125915. We thank Ferdinand Evers, Ilya Gruzberg, and Ara Sedrakyan for helpful discussions. T.V. acknowledges the hospitality of the Kavli Institute for Theoretical Physics and the Aspen Center for Physics, where part of the work was performed.

[1] K. v. Klitzing, G. Dorda, and M. Pepper, Phys. Rev. Lett. **45**, 494 (1980).
[2] P. W. Anderson, Phys. Rev. **109**, 1492 (1958).
[3] F. Evers and A. D. Mirlin, Rev. Mod. Phys. **80**, 1355 (2008).
[4] W. Li, G. A. Csáthy, D. C. Tsui, L. N. Pfeiffer, and K. W. West, Phys. Rev. Lett. **94**, 206807 (2005).
[5] W. Li, C. L. Vicente, J. S. Xia, W. Pan, D. C. Tsui, L. N. Pfeiffer, and K. W. West, Phys. Rev. Lett. **102**, 216801 (2009).
[6] A. J. M. Giesbers, U. Zeitler, L. A. Ponomarenko, R. Yang, K. S. Novoselov, A. K. Geim, and J. C. Maan, Phys. Rev. B **80**, 241411 (2009).
[7] B. Huckestein and B. Kramer, Phys. Rev. Lett. **64**, 1437 (1990).
[8] B. Huckestein, Europhys. Lett. **20**, 451 (1992).
[9] B. Huckestein, Rev. Mod. Phys. **67**, 357 (1995).
[10] D.-H. Lee and Z. Wang, Phys. Rev. Lett. **76**, 4014 (1996).
[11] Y. Huo and R. N. Bhatt, Phys. Rev. Lett. **68**, 1375 (1992).
[12] P. Cain, R. A. Römer, and M. E. Raikh, Phys. Rev. B **67**, 075307 (2003).
[13] V. V. Mkhitaryan and M. E. Raikh, Phys. Rev. B **79**, 125401 (2009).
[14] J. T. Chalker and P. D. Coddington, J. Phys. C: Solid State Phys. **21**, 2665 (1988).
[15] K. Slevin and T. Ohtsuki, Phys. Rev. B **80**, 041304 (2009).
[16] K. Slevin and T. Ohtsuki, Int. J. Mod. Phys.: Conf. Ser. **11**, 60 (2012).

[17] H. Obuse, A. R. Subramaniam, A. Furusaki, I. A. Gruzberg, and A. W. W. Ludwig, Phys. Rev. B **82**, 035309 (2010).
[18] M. Amado, A. V. Malyshev, A. Sedrakyan, and F. Dominguez-Adame, Phys. Rev. Lett. **107**, 066402 (2011).
[19] I. C. Fulga, F. Hassler, A. R. Akhmerov, and C. W. J. Beenakker, Phys. Rev. B **84**, 245447 (2011).
[20] H. Obuse, I. A. Gruzberg, and F. Evers, Phys. Rev. Lett. **109**, 206804 (2012).
[21] W. Nuding, A. Klümper, and A. Sedrakyan, Phys. Rev. B **91**, 115107 (2015).
[22] D. G. Polyakov and B. I. Shklovskii, Phys. Rev. Lett. **70**, 3796 (1993).
[23] A. M. M. Pruisken and M. A. Baranov, Europhys. Lett. **31**, 543 (1995).
[24] Z. Wang, M. P. A. Fisher, S. M. Girvin, and J. T. Chalker, Phys. Rev. B **61**, 8326 (2000).
[25] A. M. M. Pruisken and I. S. Burmistrov, JETP Lett. **87**, 220 (2008).
[26] I. S. Burmistrov, S. Bera, F. Evers, I. V. Gornyi, and A. D. Mirlin, Ann. Phys. **326**, 1457 (2011).
[27] Whereas short-range interactions are irrelevant at the non-interacting fixed point, long-range Coulomb interactions are believed to be relevant [10].
[28] I. A. Gruzberg, A. Klümper, W. Nuding, and A. Sedrakyan, Phys. Rev. B **95**, 125414 (2017).
[29] M. Ippoliti, S. D. Geraedts, and R. N. Bhatt, Phys. Rev. B **97**, 014205 (2018).
[30] Q. Zhu, P. Wu, R. N. Bhatt, and X. Wan, Phys. Rev. B **99**, 024205 (2019).
[31] R. E. Peierls, Z. Phys. **80**, 763 (1933).
[32] J. M. Luttinger, Phys. Rev. **84**, 814 (1951).
[33] D. R. Hofstadter, Phys. Rev. B **14**, 2239 (1976).
[34] R. Rammal, J. Phys. (Paris) **46**, 1345 (1985).
[35] For irrational Φ, in contrast, the spectrum consists of dense but isolated eigenvalues.
[36] L. Schweitzer, B. Kramer, and A. MacKinnon, Z. Phys. B **59**, 379 (1985).
[37] L. Schweitzer, B. Kramer, and A. MacKinnon, J. Phys. C: Solid State Phys. **17**, 4111 (1984).
[38] B. Kramer, L. Schweitzer, and A. MacKinnon, Z. Phys. B **56**, 297 (1984).
[39] For numerical stability, we also calculate γ iteratively (in 100-layer steps) by the algorithm of Refs. [37,38].
[40] Since the spectrum is symmetric with respect to $E = 0$, we consider only the positive side of the spectrum, where the lowest LL appears on the high-energy band edge.
[41] See Supplemental Material at http://link.aps.org/supplemental/10.1103/PhysRevB.99.121301 for details of the simulation parameters, the finite-size corrections at the critical point, details of the scaling analysis, and transitions in cases of non-negligible intrinsic LL width.
[42] X. Wang, Q. Li, and C. M. Soukoulis, Phys. Rev. B **58**, 3576 (1998).
[43] B. Huckestein, Phys. Rev. Lett. **72**, 1080 (1994).
[44] M. Janssen, Phys. Rep. **295**, 1 (1998).
[45] F. Evers, A. Mildenberger, and A. D. Mirlin, Phys. Rev. Lett. **101**, 116803 (2008).
[46] H. Obuse, A. R. Subramaniam, A. Furusaki, I. A. Gruzberg, and A. W. W. Ludwig, Phys. Rev. Lett. **101**, 116802 (2008).
[47] The lattice in the CC network plays a very different role than in our work. In the CC network, it represents the semiclassical electron path, whereas in our work, it defines the Hamiltonian while the electron motion is irregular.
[48] It is remarkable that the irrelevant exponent $y = 4.3(2)$ observed in Ref. [30], expected to be universal, is much larger than those found in the current work or in other recent investigations based on CC network models.
[49] It is worth emphasizing that simple manual scaling plots are not able to resolve the slowly decaying corrections in this problem.